

# Investigating groundwater flow components in an Alpine relict rock glacier (Austria) using a numerical model

Marcus Pauritsch<sup>1</sup> · Thomas Wagner<sup>2</sup> · Gerfried Winkler<sup>2</sup> · Steffen Birk<sup>2</sup>

Received: 29 February 2016 / Accepted: 12 October 2016 / Published online: 8 November 2016  
© The Author(s) 2016. This article is published with open access at Springerlink.com

**Abstract** Relict rock glaciers are complex hydrogeological systems that might act as relevant groundwater storages; therefore, the discharge behavior of these alpine landforms needs to be better understood. Hydrogeological and geophysical investigations at a relict rock glacier in the Niedere Tauern Range (Austria) reveal a slow and fast flow component that appear to be related to the heterogeneous structure of the aquifer. A numerical groundwater flow model was used to indicate the influence of important internal structures such as layering, preferential flow paths and aquifer-base topography. Discharge dynamics can be reproduced reasonably by both introducing layers of strongly different hydraulic conductivities or by a network of highly conductive channels within a low-conductivity zone. Moreover, the topography of the aquifer base influences the discharge dynamics, which can be observed particularly in simply structured aquifers. Hydraulic conductivity differences of three orders of magnitude are required to account for the observed discharge behavior: a highly conductive layer and/or channel network controlling the fast and flashy spring responses to recharge events, as

opposed to less conductive sediment accumulations sustaining the long-term base flow. The results show that the hydraulic behavior of this relict rock glacier and likely that of others can be adequately represented by two aquifer components. However, the attempt to characterize the two components by inverse modeling results in ambiguity of internal structures when solely discharge data are available.

**Keywords** Relict rock glacier · Austria · Groundwater flow · Hydraulic properties · Numerical modeling

## Introduction

Mountainous and, in particular, alpine groundwater is contributing significantly to the stream flow of rivers in valleys and consequently in the foreland (e.g., Campbell et al. 1995; Clow et al. 2003; Tague and Grant 2009; Muir et al. 2011; Welch et al. 2012). With increasing population and propagation of tourist industries and recreational activities in mountainous areas, knowledge of the hydraulic behavior and storage capacities of mountainous aquifers is getting more important for sustainable water resources management as well as for predicting natural hazards, as for example flash floods and debris flows (e.g. Lauber et al. 2014).

Especially in alpine catchments of crystalline regions, a major portion of the groundwater contributing to the streamflow originates from debris accumulations such as moraines and rock glaciers (e.g., Hood and Hayashi 2015; Wagner et al. 2016). While the hydrogeology of moraines, talus and hillslope aquifers has been the subject of intensive investigations (e.g., Clow et al. 2003; Roy and Hayashi 2009; Muir et al. 2011), knowledge about the hydraulic behavior and storage capacities of rock glaciers is sparse (Krainer and Mostler 2002; Krainer et al. 2007; Millar et al. 2013;

✉ Marcus Pauritsch  
marcus.pauritsch@edu.uni-graz.at

Thomas Wagner  
thomas.wagner@uni-graz.at

Gerfried Winkler  
gerfried.winkler@uni-graz.at

Steffen Birk  
steffen.birk@uni-graz.at

<sup>1</sup> Tannhofweg 14/8, 8044 Graz, Austria

<sup>2</sup> Institute of Earth Sciences, NAWI Graz Geocenter, University of Graz, Heinrichstrasse 26, 8010 Graz, Austria

Winkler et al. 2016a). Nevertheless, rock glaciers are common landforms all around the globe in mountainous areas and at high latitudes—for instance, in the Austrian Alps, Kellerer-Pirklbauer et al. (2012) and Krainer and Ribis (2012) have identified a total of 4,792 rock glaciers covering an area of about 286 km<sup>2</sup>. Bollmann et al. (2012) identified 1,697 rock glaciers in the South Tyrolean Alps in Italy and Schmid et al. (2015) used Google Earth to map 702 rock glaciers in selected areas of the Hindu Kush Himalayan region; therefore, rock glaciers have a high potential to influence the discharge behavior of rivers downstream of their catchments (Wagner et al. 2016).

Rock glaciers in general are scree masses that are supersaturated with ice and gravitationally move downslope with velocities of a few centimeters up to several meters per year (e.g., Barsch 1996; Haeberli et al. 2006). The size and shape of rock glaciers depends on climatic conditions, cirque geometry and debris supply of the comprising headwalls (Degenhardt 2009). Therefore, the range in size is highly variable (e.g., Kellerer-Pirklbauer et al. 2012; Krainer and Ribis 2012). The thickness of rock glaciers depends among other things on the topography of the underlying bedrock/base and is a priori difficult to estimate; however, previous investigations reported thicknesses on the order of several tens of meters (e.g., Krainer et al. 2015; Monnier and Kinnard 2015; Winkler et al. 2016a). Rock glaciers can be classified into active (currently moving), inactive (no movement, but ice is present) and relict forms (no ice mass and no movement). Active and inactive rock glaciers can also be summarized to intact rock glaciers, as both types contain ice in contrast to relict rock glaciers, where ice has melted and morphological structures such as ridges and furrows might become more obvious.

Investigations of rock glaciers mainly focus on the distribution, movement and the inner structure of intact rock glaciers (e.g., Haeberli et al. 2006; Jansen and Hergarten 2006; Leopold et al. 2011; Monnier et al. 2011). Monnier and Kinnard (2015) investigated the internal structure of an active rock glacier in the Dry Andes with ground penetrating radar. Their results suggest a heterogeneous structure with an upper and lower ice-rich layer and an intermediate zone with a high fraction of liquid water. Additionally, their results show inner structures in the form of upward-dipping reflectors caused by the movement of the rock glacier. Krainer et al. (2015) investigated an active rock glacier in the Italian Alps. They also identified a layered structure at two drill core sites on the rock glacier. Relict rock glaciers are often used as an indicator of previous permafrost conditions for climate studies (e.g., Hughes et al. 2013; Matthews and Wilson 2015), but their inner structure and hydraulic properties are largely unknown. Recently, Winkler et al. (2016a) performed hydrogeological investigations at the relict Schöneben rock glacier located in the Austrian Eastern Alps (hereinafter referred to as SRG), describing its storage and flow components

by using data of the spring hydrograph as well as natural and artificial tracers and geophysical surveys. They suggest that the rock glacier is a heterogeneous aquifer with a layered internal structure. Their investigation further suggests that there is a rather thin (approximately 10 m) layer at the base of the relict rock glacier, which consists of silty or fine sand material providing a considerable storage capacity controlling the base flow observed at the rock glacier spring (see Fig. 9 in Winkler et al. 2016a). This layer is supposed to represent glacial sediment deposits (probably morainic sediments), which would be in agreement with the findings at an active rock glacier, where moraine deposits have been encountered in two drill cores at its base (Krainer et al. 2015). The hydraulic properties of the layer at the base of the Schöneben rock glacier were additionally estimated by Pauritsch et al. (2015) using analytical models of sloping aquifers by focusing on winter base flow data. The derived hydraulic conductivity on the order of 10<sup>-5</sup> m/s is consistent with findings of Winkler et al. (2016a). The upper layers of the relict rock glacier likely consist of coarser material with a higher permeability that may explain the rapid response of the spring to recharge events. They can be activated when the lower layer is saturated or simply due to the differences of hydraulic conductivity (Winkler et al. 2016a). Another explanation might be the existence of preferential flow paths. Preferential flow paths related to cracks in the soil and roots of plants have been observed at hillslopes (e.g., Graham et al. 2010). Similarly, rapid localized flow through solution conduits is well known from karst aquifers (e.g., Worthington 2009). In this report, the term “preferential flow paths” refers to channel flow (and not layer-controlled flow); in rock glaciers, preferential flow might be possible through washed-out channels within an otherwise fine-grained layer. The existence of such channels is suggested by excavations at a relict rock glacier nearby the SRG (Untersweg and Proske 1996).

At present, a large portion of the rock glaciers are relict forms, and considering climate change (global warming), it can be assumed that today’s intact rock glaciers will also in the future become relicts. Therefore, knowledge about the hydrogeological properties of relict rock glaciers is essential for predicting future changes in the discharge behavior of rivers in alpine catchments which currently contain intact rock glaciers.

Simple lumped-parameter models are able to satisfyingly simulate the discharge behavior of complex aquifers and even of this particular relict rock glacier (Wagner et al. 2016); however, they cannot be used to investigate and distinguish between different types of heterogeneity related to the internal structure (e.g., layered structure or preferential flow paths). To resolve such a task, a distributed numerical model is preferable. Numerical models have been extensively used during the last decades and represent a helpful tool for estimating aquifer parameters (Carrera et al. 2005) and also help to improve the

conceptual understanding of a hydrogeological setting (e.g., Eisenlohr et al. 1997a, b; Mansour et al. 2012). Thus, in this report, the current conceptual understanding regarding the drainage processes within the relict Schöneben rock glacier (SRG) (Winkler et al. 2016a) is tested using a three-dimensional numerical groundwater flow model. The main purpose of this report is to indicate the major features of the internal structure (layering, draining channels, topography) controlling the discharge behavior of the relict rock glacier and to compare them with the current conceptual understanding. To this end, several model runs with increasing complexity are provided. As there are no boreholes or other information about groundwater heads, only the discharge of the draining spring is used for calibration. Due to these limitations, the attention is turned towards reproducing the discharge dynamics in general rather than the observed discharge exactly.

### Field site and data set

The investigation area in this research is the relict Schöneben rock glacier (SRG) located in the Niedere Tauern Range in Austria at E 14°40'25" and N 47°22'39" (Fig. 1). The SRG is situated in a northeast-facing alpine cirque which also represents the hydrological catchment of the SRG, covering an area of 0.67 km<sup>2</sup> with a maximum elevation of 2,295 m a.s.l. The elevation of the tongue-shaped SRG ranges from 1,715 to 1,912 m a.s.l., it has a length of about 750 m, a maximum width of about 250 m, and covers an area of 0.11 km<sup>2</sup> (Fig. 1). The surface of the SRG is covered by coarse-grained, blocky material consisting of gneissic rocks ranging from cubic decimeters to a few cubic meters. The characteristic morphology

with distinct collapse structures (i.e., caused by the melting of the ice and the resulting loss in volume), the partial vegetation cover (mainly grasses and dwarf pines) and the low slope gradient of the rock glacier front indicate that the SRG can be assumed to be a relict rock glacier, which is supported by an average water temperature above 2.2 °C at the spring emerging at the front of the rock glacier (Kellerer-Pirklbauer et al. 2015; Winkler et al. 2016a).

Steep rock faces surround the rock glacier in the eastern, southern and western area with talus slopes situated between the rock faces and the SRG itself (Fig. 1a). The catchment is drained by one large spring (hereinafter referred to as SEQ) located directly at the front of the SRG (Fig. 1a).

The SEQ is a spring belonging to the official spring network of the Hydrographic Service of Styria (HZB No. 396762). The stage is continuously monitored at a rectangular notch weir situated about 40 m downstream of the spring. Stage data have been available since July 2002 and are recorded in hourly intervals. Individual discharge measurements (using the salt dilution method) are used to relate the monitored stage to the actual discharge. Precipitation is continuously monitored at an automatic weather station located directly at the SRG at 1,822 m a.s.l. (AWS, see Fig. 1a). Precipitation data have been available since November 2011, recorded in hourly time steps.

### Model setup

The groundwater model is implemented in MODFLOW (McDonald and Harbaugh 1988) using the NWT solver (Niswonger et al. 2011; Hunt and Feinstein 2012), which

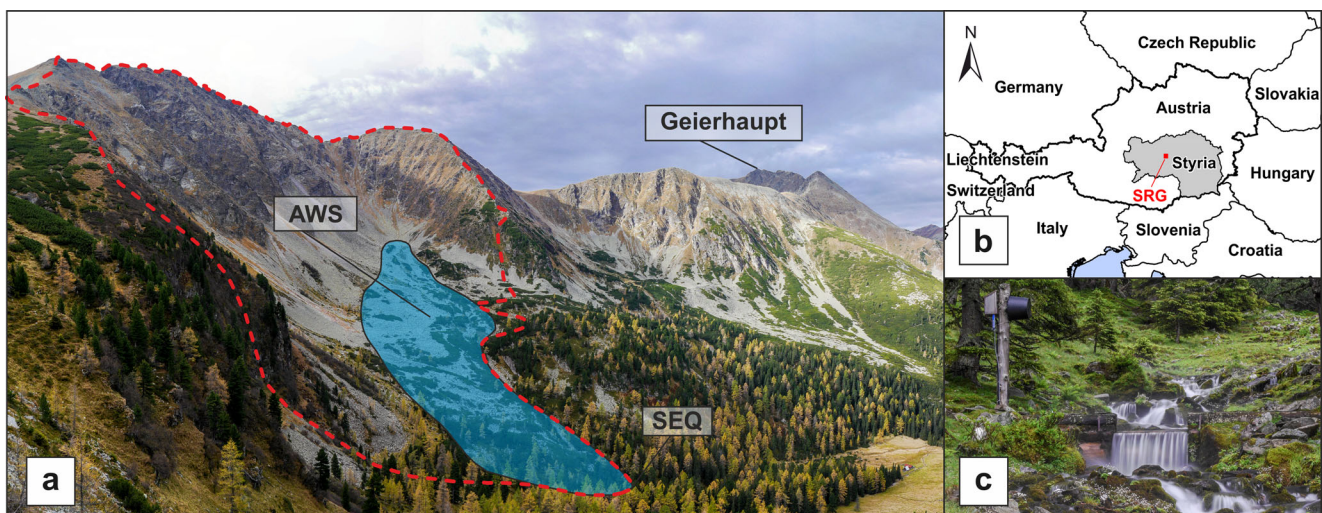


**Fig. 1** Field site impression of the Schöneben rock glacier (SRG) catchment. **a** Overview of the investigation area with the SRG highlighted in blue and the hydrological catchment delineated with a red-dashed line; AWS automatic weather station; SEQ rock glacier

spring; Geierhaupt is the highest peak in the surroundings (2,417 m a.s.l.); **b** location of the SRG within Austria and Styria; **c** rectangular notch weir situated about 40 m downstream of SEQ

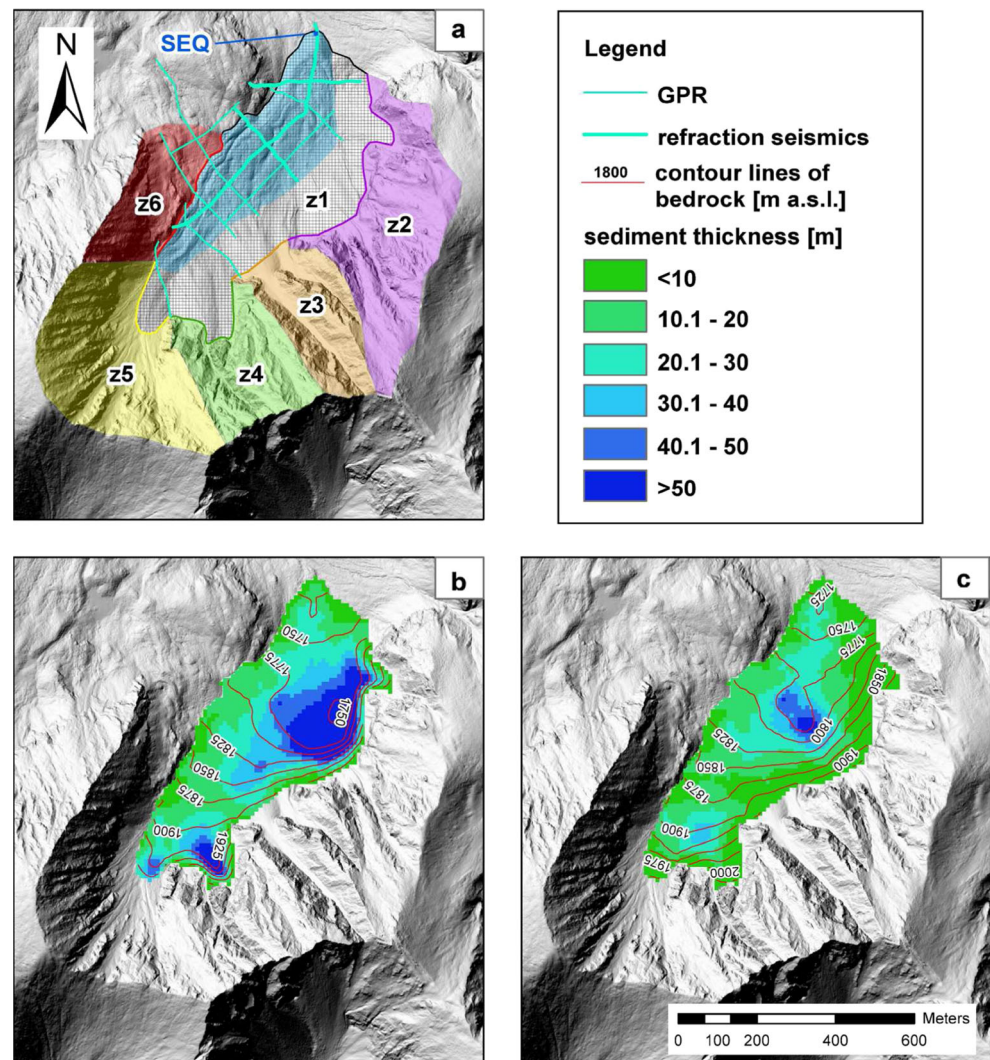


employs a Newton–Raphson solution with improved handling of dry cells. This is an important feature as the topography of the investigation area is showing a high relief, frequently causing the upper cells to fall dry. The application of other solvers, for example the PCG2 solver combined with a rewetting package, may result in an unstable model that often fails to converge.

The model domain covers an area of 225,300 m<sup>2</sup> and is set up with uniform cell sizes of 10 m × 10 m in 66 columns and 80 rows. As there is no actual boundary between the SRG and the talus slopes but rather a smooth transition, the SRG and the talus slopes are assumed to form one merged aquifer system (z1 in Fig. 2). The boundaries of the numerical model are therefore chosen to be beyond the actual boundaries of the SRG to include the adjacent talus slopes to the east and south. The boundary conditions (except for the spring and the top of the active cells) are set to no-flow boundaries as the groundwater flow through the bedrock is assumed to be negligible. Surface elevation data are adopted from a downsampled

digital elevation model (DEM) with a resolution of 10 m (based on the chosen MODFLOW cell sizes) based on airborne laser scan data (ALS) with a resolution of 1 m provided by the GIS Service of the Federal State Government of Styria (GIS Steiermark). Elevation data of the underlying bedrock are based on a digital elevation model resulting from geophysical surveys on the SRG (Fig. 2a) comprising seismic refraction investigations along three profiles (Winkler et al. 2016a) and ground penetrating radar (GPR) investigations along eight profiles (two additionally available profiles are not used herein as one of them lies outside the model area and the other is discarded due to poor data quality; see Winkler et al. 2016b). Interestingly, the results of the geophysical surveys show that the thickness of the SRG is increasing towards the southeast at the transition to the talus slopes. As the geophysical investigations did not capture the full extent of the aquifer in this part, the aquifer thickness in this area is subject to a high degree of uncertainty; therefore, two approaches were applied to determine the geometry of the aquifer base. In a first approach, the

**Fig. 2** SRG catchment with model area. **a** Cell grid and recharge zones (z1–z6) with corresponding input cells (color-coded); delineation of the actual SRG within the model area highlighted as blue polygon (see Fig. 1); profiles of geophysical investigations blue lines and constant-head cell at the spring (SEQ); **b** Color-coded sediment thickness; contour lines indicate the aquifer base topography based on geophysical data and extrapolated rock faces; **c** Color-coded sediment thickness; contour lines indicate an alternative aquifer base topography based on geophysical data and linearly decreasing depth towards the boundary



slopes of the rock faces located above the talus slopes are extrapolated below the surface and intersected with the elevation of the bedrock at the last point of the geophysical investigation profile. Including these extended profiles, the depth of the bedrock is interpolated using kriging with the software Surfer (Fig. 2b). The alternative approach uses a linear extrapolation of the geophysical profiles, i.e. the depth is assumed to decrease linearly from the last point of the profile towards the upper end of the debris slope (Fig. 2c).

It is assumed that there is no significant groundwater flow between the SRG catchment and its adjacent catchments because of the compact gneissic geology and the steep relief; moreover, groundwater storage is assumed to occur only where unconsolidated rocks are present (scree and, especially, in the relict rock glacier itself). Bare rocks and steep cliffs are assumed to have negligible storage capacities; additionally, the potential storage in the bedrock is assumed to be of minor importance as no considerable weathering zone is observable.

The recharge to the rock glacier aquifer is determined based on precipitation data from the automatic weather station located on the SRG (AWS in Fig. 1a) and an estimated evapotranspiration. The actual evapotranspiration is computed using an estimate of potential evapotranspiration based on Thomthwaite (1948) as input for a soil water balance model at a daily time step as described by, e.g., Peters et al. (2005). A relatively low value of 20 mm is used for the soil moisture storage at field capacity because the surface of the investigation area is mostly covered by coarse rock debris; moreover, the application of a simple lumped-parameter model indicated a minor role of the soil moisture accounting store (Wagner et al. 2016). The actual evapotranspiration is assumed to be equal to potential evapotranspiration if the soil moisture storage amounts at least to 70 % (14 mm) of the field capacity; below this value actual evapotranspiration is linearly decreased towards zero. Recharge occurs if the net inflow (precipitation minus actual evapotranspiration) to the soil moisture storage causes an exceedance of field capacity (time series is shown in Fig. 3).

The resulting direct recharge (i.e., precipitation falling directly onto the surface of z1 (Fig. 2a), 31 % of the total catchment area) is distributed homogeneously across the model. The recharge from the surrounding rock faces of the hydrological catchment primarily consists of surface runoff and is added to the recharge of the peripheral cells, proportional to the area percentage of the respective subcatchment (Fig. 2a). The areal percentages are 19, 10, 11, 20 and 9 % for the recharge zones z2, z3, z4, z5, and z6, respectively.

The parameter estimation software PEST (Doherty 2013) is employed for automatic calibration of the groundwater models. The hydraulic conductivity and the specific yield of specified groups of cells are treated as calibration parameters. According to the assumed plausibility of the parameter values and (in the case of the upper limit of hydraulic conductivity) to avoid model instabilities, parameter ranges between  $1 \times 10^{-2}$  and  $1 \times 10^{-7}$  m/s as well as 0.1 and 0.3 were defined for hydraulic conductivity and specific yield, respectively. The specific storage is defined as a constant value of  $1 \times 10^{-4}$  1/m. As there are no boreholes or other information about groundwater levels, the model has to be calibrated solely to the discharge of the spring (SEQ). During calibration the discharge is weighted inversely proportional to the observed values (Doherty 2013) in order to compensate for the high variability of discharge (Winkler et al. 2016a). The simulation is restricted to time periods when melting snow can be neglected in order to avoid the uncertainties involved in modeling the snow melt; therefore, the model is calibrated using the hydrograph of the SEQ in the time period from 25 June 2013 to 14 March 2014 (263 days; see Fig. 3a). This year has been chosen because it has three distinct recharge events following a long dry period, whereas the hydrograph recession of most other years is interrupted by several smaller recharge events which complicate the interpretation. The transient simulation comprises 151 stress periods and a total of 8,321 time steps with a steady-state water table as initial condition. The stationary boundary conditions are defined as constant recharge (distributed on the six recharge zones z1–z6;

**Fig. 3** Recharge and discharge ( $Q$ ) time series of **a** the calibration period and **b** the verification period. The grey area marks the warm-up period. The light blue areas mark time periods with snow influence.  $T$  time

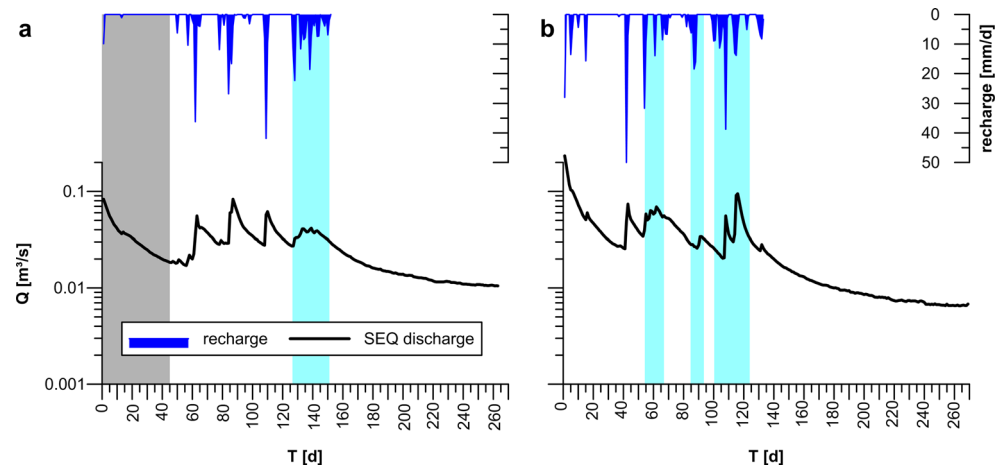


Fig. 2). The total recharge rate is thereby specified to be equal to the measured discharge at the beginning of the simulation period. In the time period from day 127 to 150, minor snowfall events occurred according to observations from an automatic digital camera monitoring the area. Because the precipitation was stored temporarily in the snow cover, the recharge occurred delayed (compared to the precipitation records at the automatic weather station) when the snow melted in the following days. As this delay is not considered in the recharge model, the time period is given only 10 % weight in the calibration. Moreover, the first 45 days of the simulation are regarded as a warm-up period (potentially affected by the initial condition) and the discharge data during that time are not used at all for calibration. Special attention is given to the accurate simulation of the winter base flow, as this time period remains unaffected by recharge events, and therefore groundwater flow components other than the base flow can be neglected; thus, the weight in the calibration during this time period is multiplied by a factor of 10. The goodness-of-fit of the model results is analyzed using the root-mean-square error (RMSE), the weighted root-mean-square error (RMSEw; see Table 1) and visual inspection of the simulated versus the observed discharge time series (neglecting the warm-up period). The model is verified by simulating the time period of 21 July 2012 to 15 April 2013 (269 days; see Fig. 3b). This time period also exhibits a winter base flow without intermediate recharge events (see Winkler et al. 2016a), and pictures of the automatic digital camera are available to identify snowfall events (Wagner et al. 2016).

In order to investigate the effects of different kinds of internal structures of the SRG and, moreover, to verify the current conceptual understanding of groundwater flow processes in relict rock glaciers, several scenarios (i–viii) with increasing complexity are simulated and compared to each other. For

these eight scenarios, the aquifer base topography with extrapolated rock faces (Fig. 2b) is applied. The model setups of the investigated scenarios in this research can be grouped in laterally homogeneous (i–iv) and heterogeneous (v–viii) models which are presented in Fig. 4. The laterally homogeneous scenarios contain models with one (i), two (ii and iii) or three (iv) layers with different hydraulic parameters for each layer. The thickness of the lower layer in ii and iii covers 20 and 80 % of the total aquifer thickness at each cell, respectively. In scenario iv the layered structure of the SRG is further refined by subdividing the lower layer of ii into two layers, each covering 10 % of the total aquifer thickness. A thin lower layer is in accordance with the current conceptual understanding of the relict SRG (Winkler et al. 2016a). Note that the upper two layers presented in Fig. 9 of Winkler et al. (2016a) are not further distinguished in the numerical models as these two layers are, compared to the lower layer, rather similar and highly conductive. Results of seismic refraction surveys showed a maximum total thickness of the rock glacier of more than 50 m (Fig. 2). However, the saturated zone was not detectable because a “blind zone” with a thickness of 19 m is possible with the applied setup of the geophysical survey, meaning that a saturated layer with a thickness of up to 19 m could have been missed in the survey (Winkler et al. 2016a and b).

In the laterally heterogeneous scenarios, a zone with higher hydraulic conductivity is introduced to models with one (v, vi) or two layers (vii, viii). This represents a washed-out channel (according to field observations/excavations from a nearby relict rock glacier; Untersweg and Proske 1996) or channel network which is lacking fine-grained material and is embedded in a less permeable (fine-grained) matrix. The orientation of the channels is defined to follow the topography of the model base and to connect the spring with one (v, vii) and five

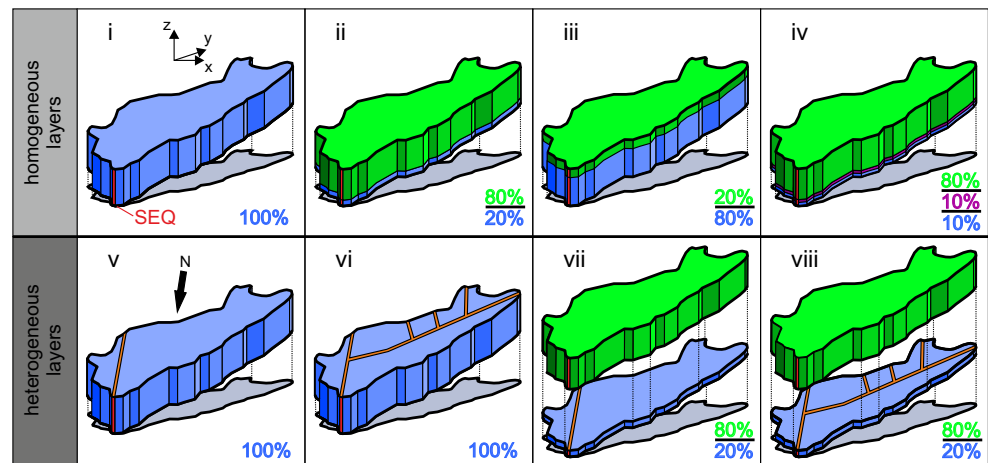
**Table 1** Estimated hydraulic parameters of the investigated scenarios and goodness-of-fit measures for the calibration period

Scenario	$K_u$ [m/s]	$K_m$ [m/s]	$K_l$ [m/s]	$K_c$ [m/s]	$SY_u$ [-]	$SY_m$ [-]	$SY_l$ [-]	$SY_c$ [-]	RMSE [m <sup>3</sup> /s]	RMSEw [m <sup>3</sup> /s]
i	$3.67 \times 10^{-4}$	–	–	–	0.30	–	–	–	$1.41 \times 10^{-2}$	$8.70 \times 10^{-3}$
ii	$5.33 \times 10^{-3}$	–	$4.93 \times 10^{-5}$	–	0.10	–	0.30	–	$1.40 \times 10^{-2}$	$4.01 \times 10^{-3}$
iii	$1.00 \times 10^{-2}$	–	$1.22 \times 10^{-5}$	–	0.21	–	0.10	–	$1.78 \times 10^{-2}$	$2.46 \times 10^{-3}$
iv	$8.00 \times 10^{-3}$	$8.00 \times 10^{-7}$	$1.70 \times 10^{-4}$	–	0.10	0.30	0.30	–	$1.38 \times 10^{-2}$	$3.17 \times 10^{-3}$
v	$2.72 \times 10^{-5}$	–	–	$1.00 \times 10^{-2}$	0.10	–	–	0.10	$9.32 \times 10^{-3}$	$5.53 \times 10^{-3}$
vi	$9.67 \times 10^{-5}$	–	–	$1.00 \times 10^{-2}$	0.17	–	–	0.10	$8.78 \times 10^{-3}$	$3.87 \times 10^{-3}$
vii	$8.61 \times 10^{-3}$	–	$3.54 \times 10^{-5}$	$2.13 \times 10^{-3}$	0.10	–	0.30	0.19	$1.44 \times 10^{-2}$	$3.08 \times 10^{-3}$
viii	$2.61 \times 10^{-3}$	–	$2.60 \times 10^{-6}$	$2.01 \times 10^{-3}$	0.22	–	0.30	0.30	$1.14 \times 10^{-2}$	$3.08 \times 10^{-3}$
ii-a	$2.02 \times 10^{-3}$	–	$7.27 \times 10^{-6}$	–	0.30	–	0.30	–	$1.33 \times 10^{-2}$	$4.49 \times 10^{-3}$
vi-a	$7.18 \times 10^{-7}$	–	–	$1.00 \times 10^{-2}$	0.17	–	–	0.10	$1.14 \times 10^{-2}$	$2.66 \times 10^{-3}$
viii-a	$3.97 \times 10^{-3}$	–	$7.29 \times 10^{-6}$	$1.59 \times 10^{-3}$	0.30	–	0.30	0.30	$1.30 \times 10^{-2}$	$4.00 \times 10^{-3}$

$K$  hydraulic conductivity,  $SY$  specific yield, subscripts:  $u$  upper-,  $m$  middle-,  $l$  lower layer;  $c$  channel;  $RMSE$  unweighted root-mean-square error;  $RMSEw$  weighted root-mean-square error



**Fig. 4** Three-dimensional sketches of the investigated internal structures of the model. Colors indicate zones with uniform hydraulic parameters within one scenario. Percentages indicate the thickness of layers. Red bars indicate the outflow cell (SEQ). Note that the actual surface and aquifer base topography is not represented here for more clarity of the sketch; color codings e.g., blue colors in i and v do not necessarily represent similar hydraulic parameters



(vi, viii) dominant gullies from outside the model area (see Fig. 2). In the two-layered scenarios (vii, viii), the channel and channel network are introduced to the lower layer (model runs with channels in both layers did not change the results). During calibration, the channel network is treated as one zone in order to minimize the number of adjustable parameters. A test run of model vi where the hydraulic parameters of the channels were individually calibrated has shown to have a nearly identical discharge behavior as one where channels were calibrated as a single zone due to a narrow range of calibrated hydraulic conductivity in the individual channels (not shown here). Furthermore, three models (ii-a, vi-a and viii-a) are presented with setups equivalent to models ii, vi and viii, but with an alternatively shaped aquifer base topography (Fig. 2c). These models are aimed to investigate to what degree the discharge behavior of the spring is affected by the morphology of the base both without and with a draining channel network.

## Results

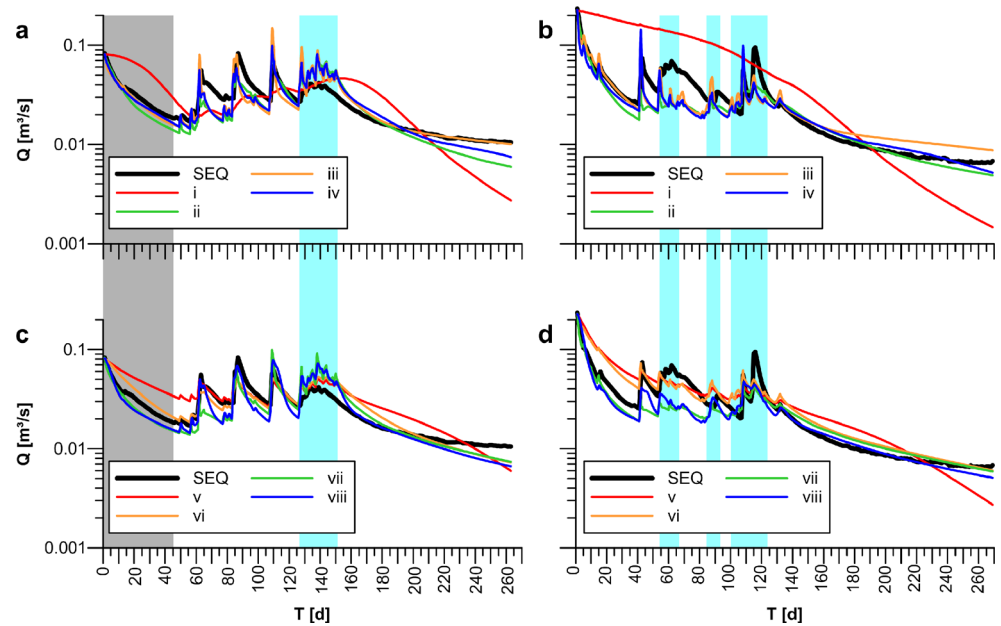
The comparisons of the simulated to the measured discharge of the SEQ in the calibration and verification periods are presented in Figs. 5 and 6. The estimated aquifer parameters and the goodness-of-fit measures RMSE and RMSEw are presented in Table 1. Some deviation between simulated and observed discharge is expected in the time period from days 127 to 150 that was less weighted in the calibration, as the recharge was affected by snow fall and snow melt processes that are not considered by the model. As a consequence, the observed discharge dynamics are not well reproduced within this period, and therefore are not further discussed; nevertheless, the following winter base flow recession appears to be largely unaffected by these short-term effects. Likewise, several snowfall and melting events occurred during the time period used for verification between days 50 and 125

(Figs. 5 and 6), resulting in delayed responses of SEQ and/or overestimated recharge as precipitation at least was partially stored in the snow cover.

Using the aquifer base topography of Fig. 2b, the results of the laterally homogeneous scenarios (Fig. 5a,b) show that the single-layered scenario i visually has a very poor fit. This is supported by the goodness-of-fit measures presented in Table 1. This scenario obviously fails to reproduce the discharge behavior of the SEQ, which is characterized by sharp peaks after recharge events and a slowly decreasing base flow. The introduction of a second homogeneous layer in scenarios ii and iii greatly improves the model fit; nevertheless, it can be seen that in ii the short-term recessions after recharge events as well as the winter base flow recessions are too fast and that the absolute value of discharge is too low between the recharge events and during the winter base flow. Scenario iii shows that with a thick lower layer, the absolute value of discharge between the recharge events is closer to the observed values. The thick lower layer also leads to higher hydraulic heads and an improved fit of the winter base flow recession in the calibration (Fig. 5a, RMSEw in Table 1) but overestimates the base flow in the verification time period (Fig. 5b). The introduction of a third layer in iv leads to similar discharge dynamics compared to ii, with similar discharge peaks but a slightly slower base flow recession. In general, the estimated aquifer parameters show a high hydraulic conductivity for the upper layer and a lower hydraulic conductivity in the lower layer (Table 1) with the single-layered scenario i showing intermediate values. Interestingly, calibration of iv results in a very low conductivity middle layer that acts as a barrier between the higher conductivity upper and lower layers.

It can be seen in Fig. 5c,d that the introduction of a draining channel to a single-layered model in v is not sufficient to represent the fast flow component of the SRG (see also Table 1). The discharge recession is generally too slow, resulting in overestimated discharge during base flow. Interestingly, the discharge recession during the winter base

**Fig. 5** Hydrographs of the investigated model scenarios compared to the observed data of *SEQ*. The *grey area* marks the warm-up period. The *light blue areas* mark time periods with snow influence. **a–b** Shows the scenarios with homogeneous layers (models i–iv in Fig. 4) for the calibration (25 June 2013 to 14 March 2014) and verification (21 July 2012 to 15 April 2013) time period, respectively. **c–d** Shows the scenarios with heterogeneous layers for the calibration and verification time period, respectively (models v–viii in Fig. 4)



flow shows a further decrease after approximately 200 days. At that time the upper part of the aquifer has fallen dry and the drying front has advanced to the area where a relatively flat basin is present in the east (see Fig. 2b). The model fit improves by extending the channel to a channel network in scenario vi; however, the simulated discharge also shows deviations to the measured discharge of the *SEQ*. While the peaks

of the major recharge events in the calibration period are close to the observed data, the discharge response to small recharge events appears too sharp and overestimated; furthermore, similar to most of the aforementioned scenarios, the long-term winter base flow is underestimated, i.e., the simulated discharge recession is too fast. In the verification period, the simulated winter base flow is close to that of the *SEQ*, but

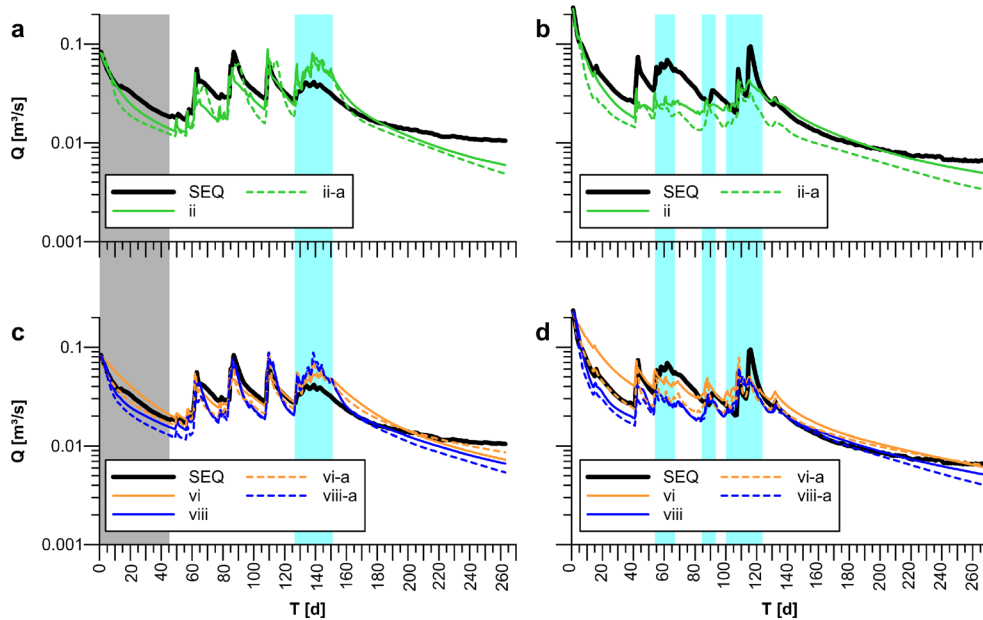


**Fig. 6** Hydrographs of the investigated model scenarios compared to the observed data of *SEQ*. The *grey area* marks the warm-up period. The *light blue areas* mark time periods with snow influence. **a–b** Shows a comparison of two laterally homogeneous layered scenarios with differently shaped topography of the model base for the calibration (25 June 2013 to 14 March 2014) and verification (21 July 2012 to 15 April 2013) time period, respectively (*solid line* refers extrapolated rock faces; see Fig. 2b);

*dashed line* is the linearly decreasing depth towards boundary (see Fig. 2c). **c–d** Shows a comparison of two laterally heterogeneous layered scenarios with differently shaped topography of the model base for the calibration and verification time period, respectively (*solid lines* are extrapolated rock faces; see Fig. 2b); *dashed lines* represent linearly decreasing depth towards boundary (see Fig. 2c)



the discharge dynamics of the preceding time period are not well matched. Scenarios vii and viii represent two-layered versions of v and vi, respectively, in which the channel and the channel network is only present in the lower layer (see Fig. 4). The hydrograph of vii is similar to that of ii, indicating that the upper layer is dominating the quick flow component rather than the channel. The channel network of viii obviously has a larger influence than the single channel in vii and results in a quickly responding hydrograph but with broad peaks (resulting in a slightly better RMSE, but identical RMSE<sub>w</sub>, Table 1). Moreover, the base flow between the recharge events and the winter base-flow recession are similar to the layered scenarios ii, iii and vii.

Examining the results of the scenarios using the alternatively shaped model base (Fig. 2c) shows that the topography of the base has some influence on the discharge behavior of the homogeneous layered model. As can be seen during the calibration (Fig. 6a), ii-a shows double peaks at the major recharge events. In the verification time series (Fig. 6b) the double peaks cannot be observed and the discharge dynamics of ii-a appear more realistic than ii, although the absolute discharge is underestimated. Using the alternatively shaped base (Fig. 2c) results in a winter recession approximately following an exponential decrease (Fig. 6a,b). The heterogeneous layered scenarios vi-a and viii-a visually only slightly differ from vi and viii, respectively (Fig. 6c,d), but yield higher RMSE values (indicating an inferior fit) and different parameter estimates (Table 1). While the matrix of vi-a has a lower hydraulic conductivity compared to vi, the matrix of the lower layer of viii-a has a higher hydraulic conductivity and specific yield compared to viii.

## Discussion

The model results indicate that this aquifer has at least two domains with different aquifer properties. This finding is in good agreement with the outcomes of Winkler et al. (2016a), who used spring data as well as natural and artificial tracers to show that the relict Schöneben rock glacier is a heterogeneous aquifer with an assumed layered structure. Importantly, this investigation indicates that both scenarios, one with a layered internal structure and the other with an internal structure with draining channels, can simulate the fast and slow groundwater flow components that were shown to exist in the previous studies (Wagner et al. 2016; Winkler et al. 2016a). Moreover, the numerical modeling exercise supports the existence of a rather thin lower layer with low hydraulic conductivity, which might include channels with a high hydraulic conductivity; however, the findings cannot give a clear preference to one of the investigated internal structures.

If both a layered structure and channels exist, the discharge behavior is dependent on the extent of the channel network.

With a single channel (vii), the discharge is dominated by the layered structure, and the channel only plays a subordinate role (Fig. 5c,d). With a network of channels in the lower layer (viii) the influence of the channels increases. Scenarios vii and viii (Fig. 4) illustrate that both types of heterogeneity influence the discharge behavior in a different way. The different extent of the draining channels mainly affects the fit of the discharge peaks and the short-term runoff after recharge events. In contrast, the base flow between the recharge events and the winter base flow is similar in both scenarios and also similar to the corresponding scenario without channels; therefore, the base flow is dominated by the layered structure rather than by the draining channels.

According to the conceptual model of the relict rock glacier of Winkler et al. (2016a) and drill core observations of Krainer et al. (2015), the basal layer might represent morainic remnants. As this layer was not detectable in the geophysical investigations at the SRG, there is no information about the lateral distribution and extension of this layer. Excavations at the neighboring Hochreichart Rock Glacier showed that there is a washed-out zone in the proximity of the spring that is lacking fine-grained material (Untersweg and Proske 1996) and therefore has a high hydraulic conductivity. Thus, it might be reasonable to assume that this layer is not homogeneously distributed across the aquifer. Assuming slow development processes of a talus-derived rock glacier, preexisting water flow paths or newly evolving ones will probably prevent sedimentation of fine-grained sediments or wash them out, therefore leaving a channel network of unknown extent between patchily distributed sediment accumulations of lower hydraulic conductivity. Graham et al. (2010) showed at excavations of a hillslope watershed that a network of preferential flow paths occurred at the soil-bedrock boundary, which was controlled by the bedrock topography. Scenario vi shows that with such a channel network even a single-layered model can reproduce the discharge dynamics of the SEQ reasonably well, and the fit of the simulated hydrograph could be even further optimized by adjusting the number and extent of the channels. Yet, this would suggest a matrix hydraulic conductivity of about  $10^{-4}$ – $10^{-5}$  m/s, which is in discrepancy with the geophysical investigations, suggesting coarse-grained sediments based on seismic velocities. Moreover, fine-grained sediments, for instance from the development, evolution, and movement of the rock glacier itself, are likely to exist as a potential source of low conductive zones (e.g., Zurawek 2002; Hausmann et al. 2012).

As a saturated zone needs to exist within the rock glacier to provide groundwater (especially base flow) for the spring, the thickness of the saturated zone is estimated to be around 10–15 m based on recession analysis but seems to be limited to a maximum thickness of 19 m based on refraction seismic results (see Fig. 9 in Winkler et al. 2016a). However, as can be seen in Fig. 5a, model setups containing thin lower layers lead

to an underestimation of the base flow between the major recharge events as well as during the winter base flow recession in the calibration period. Keeping in mind that the specific yield of the thin lower layers is always calibrated to 0.3, which was specified as the upper limit of realistic values (see Table 1), this result indicates that the storage of a thin lower layer is not sufficient to reproduce the observed discharge during base flow conditions, which might be related to the simplified aquifer base topography of the model.

The comparison of the scenarios with differently shaped aquifer bases in Fig. 6 shows that even though a large part of the aquifer is identical (see Fig. 2), the different aquifer base topographies and the resulting differences in aquifer thickness cause changes of the discharge dynamics or the estimated aquifer parameters. Because of the higher sediment thickness, scenario ii shows a slower recession and higher base flow relative to ii-a (Fig. 6a,b). Similarly, the lower thickness of the lower layer of vi-a compared to vi (Fig. 2) results in a slightly faster recession between the major recharge events. However, due to the higher number of adjustable parameters in the more complex scenarios (viii and viii-a), the effect of the different sediment thickness can be compensated by changes of the hydraulic parameters; hence, the role of the base topography appears to be more important in the less complex scenarios.

According to these results, for the SRG the modeled aquifer base topography based on the extrapolated rock faces in the eastern part of the model area seems more likely, because the higher thicknesses result in a higher storage capacity, which is preferable to simulate the observed base flow. The estimated hydraulic conductivity of the SRG (Table 1) is in good agreement with findings of Pauritsch et al. (2015) and Winkler et al. (2016a). Nevertheless, the winter base flow cannot be reproduced correctly in the calibration period with either of the applied aquifer bases. Remarkably, the base flow recession in the verification period is better matched by the scenarios containing the thin base layer, but even here the models tend to underestimate base flow at the late stage. The observed winter base flow clearly deviates from a single exponential recession. In fact, from 10 days onward the recession is found to follow a power law (Winkler et al. 2016a). The simulated recession curves also deviate from an exponential recession (which would be a straight line in the semi-log plots shown in Figs. 5 and 6), but not as much as the observed discharge. Conceptually, a fractal size distribution of storage elements has been proposed to explain the power law recession of spring hydrographs (Hergarten and Birk 2007), which suggests that the assumption of homogeneous layers might be oversimplified and discontinuities should be considered. In particular, the assumption of heterogeneous layers with spatially varying thickness could provide a larger storage compared with the model setups considered here and still be consistent with the results from the geophysical investigations that covered only parts of the aquifer.

Another explanation for the discrepancies of the simulated and observed base flow might be the influence of the vadose zone, which was not considered in the models; however, because of the coarse blocky debris and its low retention capabilities, precipitation can instantaneously infiltrate through the top layer of the rock glacier. Precipitation is therefore assumed to quickly pass through the unsaturated zone to become groundwater recharge. This is supported by the findings of the tracer test conducted in 2012 (Winkler et al. 2016a), where the tracer, injected at a distance of 350 m from the spring at the surface of the rock glacier, was detected after 2–3 h at the spring. In addition, Wagner et al. (2016) showed that parameters of a simple lumped-parameter model indicate a rather fast transfer of seepage water towards the saturated zone (time parameter  $x_4$  in Wagner et al. 2016). Furthermore, it was assumed in the model that the contribution of the mountain block recharge, i.e., groundwater flow out of the bedrock of the contributing catchment into the rock glacier (e.g., Welch et al. 2012), is negligible in such a crystalline catchment with an insignificant weathering zone. Assuming an additional constant inflow from the bedrock (mountain block recharge), a slightly better model fit to the winter base flow is conceivable. However, as this would have little effect on the discharge dynamics and as there is no data or field evidence of such a flow component, such a more complex model was not considered herein.

More plausible explanations for the discrepancies of the simulated and measured discharge might be unrealistic initial conditions and/or underestimated recharge. The influence of the initial condition could be further reduced by extending the simulation to perennial time periods, but this would require the introduction of a snow model, thus leading to more adjustable parameters. An underestimation of the recharge might result from the general uncertainties in the measurement of precipitation in alpine terrains. Wagner et al. (2016) demonstrated that a lumped-parameter model is able to simulate the perennial discharge behavior of the SRG reasonably well, but only when additional water is considered (water exchange coefficient  $x_2$  in Wagner et al. 2016) to compensate for water balance deficits. In the numerical groundwater model, such water balance deficits were not compensated and thus are likely to account at least partly for the deviation of the simulated from the observed discharge. As a consequence, the most complex model structures considered here do not perform much better than the less complex models (apart from the most simple single-layer scenario). A simple lumped-parameter model as employed by Wagner et al. (2016) therefore might be an appropriate choice for predictive hydrological modeling. In this study, however, the modeling is aimed at supporting the aquifer characterization, which requires a process-based groundwater model.

In the absence of spatial information about hydraulic heads, the calibration of the groundwater model solely relies on

spring discharge and therefore leads to ambiguous results, in particular with regard to the distribution of fine-grained sediments and preferential flow paths. Nevertheless, the results of the present modeling study are helpful for the design of future investigation and monitoring campaigns. As the installation of piezometers is technically difficult and expensive, the use of additional geophysics seems more beneficial. Based on the outcome of the modeling scenarios, more precise information about the distribution and thickness of the fine-grained sediments, which are assumed to exist as a thin (<19 m) layer at the base of the aquifer, is paramount. For this task, additional refraction seismic investigations with adjusted setups (narrower geophone distance) seem to be particularly promising. In addition, an extension of the previously conducted investigation towards southeast would be of great help, as this area appears to provide the highest thickness of the sediments and, thus, potentially high storage that may account for the observed recession base flow.

There are several other methods that could be envisaged for future investigations, but each of them has some drawbacks that need to be considered as well. Additional ground-penetrating radar measurements (GPR) can be applied considering varying frequencies (especially lower ones) to improve the existing data. Similar results related to challenging GPR data were shown by Merz et al. (2015) who addressed the high level of noise (especially in areas with low ice contents) to interferences caused by the boulders of the surface layer and shallow heterogeneities; however, they have shown that airborne ground-penetrating radar (antenna mounted on a helicopter) greatly improves the quality of the data. Also other airborne geophysical methods such as frequency-domain or time-domain electromagnetics might help to gain further insights; nevertheless, all airborne methods prefer constant elevation above ground (De Barros and Guimaraes 2016), which can be challenging in alpine terrain. Electrical resistivity tomography might be a cost-effective solution, but the coarse blocky material at the surface of relict rock glaciers results in a weak electrode coupling to the ground. Furthermore, the extended, air filled voids, and the lack of mineral soils or ice lead to weak electrical contacts between the individual blocks which makes the application of this method rather challenging (Hilbich et al. 2009; Kellerer-Pirklbauer et al. 2014); however, capacitively coupled resistivity methods, which use an alternating current across a transmitter-earth capacitor, can be used as an alternative to overcome these (Hauck 2013).

Thus, characterizing the hydrogeological properties and functioning of rock glaciers remains a challenging but important task. Rock glaciers represent significant aquifers in alpine catchments and are the source of many important water basins (e.g., Wagner et al. 2016). Furthermore, high heavy metal concentrations within the melt water of an active rock glacier recently reported by Krainer et al. (2015) illustrate the vulnerability of these aquifers to contamination. In addition, rock

glaciers are potentially affected by impacts of the future global warming. Assessing groundwater flow and transport processes in a changing environment is particularly challenging. While purely empirical models are considered inadequate for accomplishing this task (e.g., Rehl and Birk 2010), further progress in the hydrogeological characterization of rock glaciers is needed to reduce the ambiguity of the calibration of process-based distributed models. The afore-mentioned findings provide a guideline towards the further investigation of the rock glacier considered here that can likely be transferred to similar settings elsewhere.

## Conclusions

A number of model scenarios representing the relict SRG have been elaborated using a numerical groundwater flow model. Several scenarios differing in the internal structure and the topography of the aquifer base were considered to indicate the major features that control the discharge behavior of the rock glacier spring. The results of this modeling study converge to a consistent conceptual understanding of the hydrological functioning of the rock glacier. It has been found that two aquifer components are necessary to account for the observed discharge behavior: a highly conductive layer and/or channel network controlling the fast and flashy spring responses to recharge event, as opposed to less conductive sediment accumulations sustaining the long-term base flow. Despite the ambiguity of the specific implementation, the parameter estimates obtained from the model calibration provide order-of-magnitude estimates of the hydraulic properties of these two components. The hydraulic conductivity of the highly conductive component is found to be on the order of  $10^{-2}$ – $10^{-3}$  m/s, whereas the hydraulic conductivity of the low-conductivity elements is about three orders-of-magnitude less. The specific yield of the high-conductivity elements varied between the different model setups. Assuming a low-conductivity layer at the aquifer base covering 20 % of the total thickness, the specific yield of this layer is consistently 0.3, which corresponds to the upper limit assumed to be plausible. As the long-term base flow is underestimated by most of the model scenarios, the specific yield or the thickness of this layer might be even larger than assumed here.

The topography of the aquifer base is found to have an impact on the discharge behavior particularly when a simple internal structure is considered. If more complex aquifer structures with a high number of adjustable parameters are employed, changes in the topography can be compensated by the adjustment of other parameters. This ambiguity can only be resolved if additional data are included as constraint on the aquifer properties and internal structure (especially further geophysical investigations) or as additional calibration target (e.g., hydraulic heads).



The Schöneben Rock Glacier in the Niedere Tauern Range, Austria, is one example of a relict rock glacier and its hydrological functioning might be representative for other relict rock glaciers as well. Thus, the insights obtained herein will have implications for intact rock glaciers in the course of climate warming and future investigations of contaminant transport in rock glaciers. As such, studying the discharge behavior of relict rock glaciers (and other alpine debris accumulations) contributes largely to a better understanding of the complex hydrological processes in alpine regions and of their contribution to the fragile ecological systems in such environments.

**Acknowledgments** Open access funding provided by University of Graz. This study was funded by the European Regional Development Fund (ERDF) and the Federal State Government of Styria. The authors are grateful to the Hydrographic Service of Styria for providing the discharge data. The digital elevation models and the topographic maps were provided by the GIS Service of the Federal State Government of Styria (GIS Steiermark). We acknowledge the constructive suggestions by Majdi Mansour, an anonymous reviewer and the associate editor Alan MacDonald, which greatly improved the report.

**Open Access** This article is distributed under the terms of the Creative Commons Attribution 4.0 International License (<http://creativecommons.org/licenses/by/4.0/>), which permits unrestricted use, distribution, and reproduction in any medium, provided you give appropriate credit to the original author(s) and the source, provide a link to the Creative Commons license, and indicate if changes were made.

## References

- Barsch D (1996) Rockglaciers: indicators for the present and former geocology in high mountain environments. Springer Series in Physical Environment 16, Springer, Heidelberg, Germany
- Bollmann E, Rieg L, Spross M, Sailer R, Bucher K, Maukisch M, Monreal M, Zischg A, Mair V, Lang K, Stötter, J (2012) Blockgletscherkataster Südtirol: Erstellung und Analyse [Rock glacier registry South Tyrol: creation and analysis]. Innsbrucker Geographische Studien 39, Permafrost in Südtirol, IGS, Innsbruck, Austria, pp 147–171
- Campbell DH, Clow DW, Ingersoll GP, Mast MA, Spahr NE, Turk JT (1995) Processes controlling the chemistry of two snowmelt-dominated streams in the Rocky Mountains. *Water Resour Res* 31(11):2811–2821. doi:10.1029/95WR02037
- Carrera J, Alcolea A, Medina A, Hidalgo J, Slooten LJ (2005) Inverse problem in hydrogeology. *Hydrogeol J* 13(1):206–222. doi:10.1007/s10040-004-0404-7
- Clow DW, Schrott L, Webb R, Campbell DH, Torizzo A, Dornblaser M (2003) Ground water occurrence and contributions to streamflow in an Alpine catchment, Colorado Front range. *Ground Water* 41:937–950. doi:10.1111/j.1745-6584.2003.tb02436.x
- De Barros CE, Guimaraes SNP (2016) Magnetic airborne survey: geophysical flight. *Geosci Instrum Method Data Syst* 5:181–192. doi:10.5194/gi-5-181-2016
- Degenhardt JJ (2009) Development of tongue-shaped and multilobate rock glaciers in alpine environments: interpretations from round penetrating radar surveys. *Geomorphology* 109(3–4):94–107. doi:10.1016/j.geomorph.2009.02.020
- Doherty J (2013) PEST: model-independent parameter estimation, user manual. Watermark Numerical Computing, Brisbane, Australia. <http://www.pesthomepage.org/downloads.php>. Accessed October 2016
- Eisenlohr L, Bouzelboudjen M, Király L, Rossier Y (1997a) Numerical versus statistical modelling of natural response of a karst hydrogeological system. *J Hydrol* 202(1–4):244–262. doi:10.1016/S0022-1694(97)00069-3
- Eisenlohr L, Király L, Bouzelboudjen M, Rossier Y (1997b) Numerical simulation as a tool for checking the interpretation of karst spring hydrographs. *J Hydrol* 193(1–4):306–315. doi:10.1016/S0022-1694(96)03140-X
- Graham CB, Woods RA, McDonnell JJ (2010) Hillslope threshold response to rainfall: (1) a field based forensic approach. *J Hydrol* 393(1–2):65–76. doi:10.1016/j.jhydrol.2009.12.015
- Haeberli W, Hallet B, Arenson L, Elconin R, Humlum O, Kääb A, Kaufmann V, Ladanyi B, Matsuoka N, Springman S, Mühl DV (2006) Permafrost creep and rock glacier dynamics. *Permafr Periglac Process* 17:189–214. doi:10.1002/ppp.561
- Hauck C (2013) New concepts in geophysical surveying and data interpretation for permafrost terrain. *Permafr Periglac Process* 24:131–137. doi:10.1002/ppp.1774
- Hausmann H, Krainer K, Brückl E, Ulrich C (2012) Internal structure, ice content and dynamics of Ölgrube and Kaiserberg rock glaciers (Ötztal Alps, Austria) determined from geophysical surveys. *Aust J Earth Sci* 105(2):12–31
- Hergarten S, Birk S (2007) A fractal approach to the recession of spring hydrographs. *Geophys Res Lett* 34, L11401. doi:10.1029/2007GL030097
- Hilbich C, Marescot L, Hauck C, Loke MH, Mäusbacher R (2009) Applicability of electrical resistivity tomography monitoring to coarse blocky and ice-rich permafrost landforms. *Permafr Periglac Proc* 20:269–284. doi:10.1002/ppp.652
- Hood JL, Hayashi M (2015) Characterization of snowmelt flux and groundwater storage in an alpine headwater basin. *J Hydrol* 521:482–497. doi:10.1016/j.jhydrol.2014.12.041
- Hughes PD, Gibbard PL, Ehlers J (2013) Timing of glaciation during the last glacial cycle: evaluating the concept of a global ‘Last Glacial Maximum’ (LGM). *Earth Sci Rev* 125:171–198. doi:10.1016/j.earscirev.2013.07.003
- Hunt RJ, Feinstein DT (2012) MODFLOW-NWT: robust handling of dry cells using a Newton formulation of MODFLOW-2005. *Ground Water* 50:659–663. doi:10.1111/j.1745-6584.2012.00976.x
- Jansen F, Hergarten S (2006) Rock glacier dynamics: stick-slip motion coupled with hydrology. *Geophys Res Lett* 33, L10502. doi:10.1029/2006gl026134
- Kellerer-Pirklbauer A, Lieb KG, Kleinfürchner H (2012) A new rock glacier inventory of the Eastern European Alps. *Aust J Earth Sci* 105(2):78–93
- Kellerer-Pirklbauer A, Pauritsch M, Morawetz R, Kuehnast B, Schreiechler M, Winkler G (2014) Thickness and internal structure of relict rock glaciers: a challenge for geophysics: examples from two rock glaciers in the Eastern Alps. *Geophys Res Abstr* 16:EGU2014–EGU12581
- Kellerer-Pirklbauer A, Pauritsch M, Winkler G (2015) Widespread occurrence of ephemeral funnel hoarfrost and related air ventilation in coarse-grained sediments of a relict rock glacier in the Seckauer Tauern Range, Austria. *Geogr Ann A* 97(3):453–471. doi:10.1111/geoa.12087
- Krainer K, Mostler W (2002) Hydrology of active rock glaciers: examples from the Austrian Alps. *Arc Antarc Alp Res* 34:142–149. doi:10.2307/1552465
- Krainer K, Ribis M (2012) A rock glacier inventory of the Tyrolean Alps (Austria). *Aust J Earth Sci* 105(2):32–47
- Krainer K, Mostler W, Spoetl C (2007) Discharge from active rock glaciers, Austrian Alps: a stable isotope approach. *Aust J Earth Sci* 100:102–112

- Krainer K, Bressan D, Dietre B, Haas JN, Hajdas I, Lang K, Mair V, Nickus U, Reidl D, Thies H, Tonidandel D (2015) A 10,300-year-old permafrost core from the active rock glacier Lazaun, southern Ötztal Alps (South Tyrol, northern Italy). *Quat Res* 83(2):324–335. doi:10.1016/j.yqres.2014.12.005
- Lauber U, Kotyla P, Morche D, Goldscheider N (2014) Hydrogeology of an Alpine rockfall aquifer system and its role in flood attenuation and maintaining baseflow. *Hydrol Earth Syst Sci* 18:4437–4452. doi:10.5194/hess-18-4437-2014
- Leopold M, Williams MW, Caine N, Völkel J, Dethier D (2011) Internal structure of the Green Lake 5 rock glacier, Colorado Front Range, USA. *Permafrost Periglac* 22:107–119. doi:10.1002/ppp.706
- Mansour MM, Hughes AG, Robins NS, Ball D, Okoronkwo, C (2012) The role of numerical modelling in understanding groundwater flow in Scottish alluvial aquifers. In: Shepley MG (ed) *Groundwater resources modelling: a case study from the UK*. Geol Soc London Spec Publ 364:85–98
- Matthews JA, Wilson P (2015) Improved Schmidt-hammer exposure ages for active and relict pronival ramparts in southern Norway, and their palaeoenvironmental implications. *Geomorphology* 246: 7–21. doi:10.1016/j.geomorph.2015.06.002
- McDonald MG, Harbaugh AW (1988) A modular three-dimensional finite-difference ground-water flow model. *US Geol Surv Tech Water Resour Invest* 6-A1, 586 pp
- Merz K, Maurer H, Buchli T, Horstmeyer H, Green AG, Springman SM (2015) Evaluation of ground-based and helicopter ground-penetrating radar data acquired across an Alpine Rock Glacier. *Permafrost Periglac* 26:13–27. doi:10.1002/ppp.1836
- Millar CI, Westfall RD, Delany DL (2013) Thermal and hydrologic attributes of rock glaciers and periglacial talus landforms: Sierra Nevada, California, USA. *Quat Int* 310:169–180. doi:10.1016/j.quaint.2012.07.019
- Monnier S, Kinnard C (2015) Internal structure and composition of a Rock Glacier in the Dry Andes, inferred from ground-penetrating radar data and its artefacts. *Permafrost Periglac Proc* 26(4):335–346. doi:10.1002/ppp.1846
- Monnier S, Camerlunck C, Rejiba F, Kinnard C, Feuillet T, Dhemaïed A (2011) Structure and genesis of the Thabor rock glacier (Northern French Alps) determined from morphological and ground-penetrating radar surveys. *Geomorphology* 134:269–279. doi:10.1016/j.geomorph.2011.07.004
- Muir DL, Hayashi M, McClymont AF (2011) Hydrological storage and transmission characteristics of an alpine talus. *Hydrol Process* 25: 2954–2966. doi:10.1002/hyp.8060
- Niswonger RG, Pandai S, Ibaraki M (2011) MODFLOW-NWT: a Newton formulation for MODFLOW-2005. *US Geol Surv Tech Methods* 6-A37, 44 pp
- Pauritsch M, Birk S, Wagner T, Hergarten S, Winkler G (2015) Analytical approximations of discharge recessions for steeply sloping aquifers in alpine catchments. *Water Resour Res* 51: 8729–8740. doi:10.1002/2015WR017749
- Peters E, Van Lanen HAJ, Torfs PJJF, Bier G (2005) Drought in groundwater: drought distribution and performance indicators. *J Hydrol* 306(1–4):302–317. doi:10.1016/j.jhydrol.2004.09.014
- Rehr C, Birk S (2010) Hydrogeological characterisation and modelling of spring catchments in a changing environment. *Aust J Earth Sci* 103(2):106–117
- Roy JW, Hayashi M (2009) Multiple distinct groundwater flow systems of single moraine-talus feature in alpine watershed. *J Hydrol* 373: 139–150. doi:10.1016/j.jhydrol.2009.04.018
- Schmid MO, Baral P, Gruber S, Shahi S, Shrestha T, Stumm D, Wester P (2015) Assessment of permafrost distribution maps in the Hindu Kush Himalayan region using rock glaciers mapped in Google Earth. *Cryosphere* 9:2089–2099. doi:10.5194/tc-9-2089-2015
- Tague C, Grant GE (2009) Groundwater dynamics mediate low-flow response to global warming in snow-dominated alpine regions. *Water Resour Res* 45, W07421. doi:10.1029/2008wr007179
- Thornthwaite CW (1948) An approach towards a rational classification of climate. *Geogr Rev* 38:55–94. doi:10.1097/00010694-194807000-00007
- Untersweg T, Proske H (1996) Untersuchungen an einem fossilen Blockgletscher im Hochreichhartgebiet (Niedere Tauern, Steiermark) [Investigations at a relict rock glacier in the Hochreichhart area “Niedere Tauern Range, Styria”]. *Grazer Schrift Geogr Raumfor* 33:201–207
- Wagner T, Pauritsch M, Winkler G (2016) Impact of relict rock glaciers on spring and stream flow of alpine watersheds: examples of the Niedere Tauern Range, Eastern Alps (Austria). *Aust J Earth Sci* 109. doi:10.17738/ajes.2016.0006
- Welch LA, Allen DM, van Meerveld HJ (2012) Deep groundwater contributions to mountain headwater streams and sensitivity to available recharge. *Can Water Resour J* 37(4):349–371. doi:10.4296/cwrj3703907
- Winkler G, Wagner T, Pauritsch M, Birk S, Kellerer-Pirkelbauer A, Benischke R, Leis A, Morawetz R, Schreilechner MG, Hergarten S (2016a) Identification and assessment of flow and storage components of the relict Schöneben Rock Glacier, Niedere Tauern Range, Eastern Alps (Austria). *Hydrogeol J* 24:937–953. doi:10.1007/s10040-015-1348-9
- Winkler G, Pauritsch M, Wagner T, Kellerer-Pirkelbauer A (2016b) Reliktische Blockgletscher als Grundwasserspeicher in alpinen Einzugsgebieten der Niederen Tauern [Relict rock glaciers as groundwater storages in alpine catchment areas in the Niedere Tauern Range]. *Berichte zur wasserwirtschaftlichen Planung Steiermark*, vol 87. Graz, 134 pp. [http://www.wasserwirtschaft.steiermark.at/cms/dokumente/11913323\\_102332494/6885027d/87.pdf](http://www.wasserwirtschaft.steiermark.at/cms/dokumente/11913323_102332494/6885027d/87.pdf). Accessed 12 September 2016
- Worthington SRH (2009) Diagnostic hydrogeologic characteristics of a karst aquifer (Kentucky, USA). *Hydrogeol J* 17:1665–1678. doi:10.1007/s10040-009-0489-0
- Zurawek R (2002) Internal structure of a relict rock glacier, Ślęza Massif, southwest Poland. *Permafrost Periglac Process* 13:29–42. doi:10.1002/ppp.403